Journal of Colloid and Interface Science 337 (2009) 218–226

Contents lists available at ScienceDirect

Journal of Colloid and Interface Science

www.elsevier.com/locate/jcis

Small-angle neutron scattering study of shearing effects on drag-reducing surfactant solutions

Yunying Qi [a], Kenneth Littrell [b], Pappannan Thiyagarajan [c], Yeshayahu Talmon [d], Judith Schmidt [d], Zhiqing Lin [a], Jacques L. Zakin [a,*]

[a] The Department of Chemical and Biomolecular Engineering, The Ohio State University, Columbus, OH 43210, USA
[b] Oak Ridge National Laboratory, MS 6393 Oak Ridge, TN 37831-6393, USA
[c] Office of Basic Energy Sciences, U.S. Dept. of Energy, 1000 Independence Ave., SW, Washington, DC 20585, USA
[d] Department of Chemical Engineering, Technion-Israel Institute of Technology, Haifa 32000, Israel

ARTICLE INFO

Article history:
Received 23 January 2009
Accepted 7 May 2009
Available online 18 May 2009

Keywords:
Surfactant
Drag reduction
Rheology
SANS (small-angel neutron scattering)

ABSTRACT

Drag-reducing surfactant solutions are very sensitive to shear. Shear can induce nanostructural transitions which affect drag reduction effectiveness and rheological properties. Literature reports on the effects of shear on different micellar solutions are inconsistent. In this paper, the effects of shear on three cationic drag-reducing surfactant solutions each with very different nanostructures and rheological behaviors, Arquad 16-50/sodium salicylate (NaSal) (5 mM/5 mM) (has thread-like micelles, shear-induced structure and large first normal stress (N_1)), Arquad S-50/NaSal (5 mM/12.5 mM) (has branched micelles, no shear-induced structure and first normal stress is about zero) and Arquad 16-50/sodium 3,4-dimethyl-benzoate (5 mM/5 mM) (has vesicles and thread-like micelles, shear-induced structure and high first normal stress (N_1)) are studied by small-angle neutron scattering (SANS), together with their rheological properties, drag reduction behavior and nanostructures by cryogenic-temperature transmission electron microscopy(cryo-TEM). The differences in the rheological behavior and the SANS data of the solutions are explained by the different responses of the nanostructures to shear based on a two-step response to shear.

1. Introduction

Drag reduction is a turbulent flow phenomenon by which small amounts of drag-reducing additives can greatly reduce the friction factors of a turbulent flow [1]. High molecular weight polymers and surfactants are the two most commonly used drag-reducing additives. In the latter case, it is generally accepted that the effect is caused by the existence of long thread-like nanostructures which can provide reductions in pumping energy of up to 90% [2]. In the past few decades significant advances have been made in understanding thread-like aggregates of surfactant solution systems. These developments are reviewed in Ref. [1,2]. Although polymer additives can also provide high drag reduction, they are not suitable for use in recirculation systems as the high molecular weight species present degrade irreversibly under mechanical shear encountered in pumps. Dilute drag-reducing surfactant solutions are also very sensitive to shear and lose their effectiveness at high shear stress, but, in contrast to polymers, they recover in seconds after mechanical degradation because of the self-assembling nature of their micelles and therefore are well-suited for recirculation systems such as district heating and cooling systems [1].

The effects of shear on surfactant solutions have been studied by rheology, dynamic light scattering and small-angle neutron scattering (SANS) for example [3–6]. In their investigations of the structural aspects of micelles with SANS, Mendes and Menon [5] and Mendes et al. [6] reported that vesicles, which are closed bilayers or multilayers of surfactants, transform to thread-like micelles under shear in a drag-reducing surfactant solution which explained their surprising observation of an effective drag-reducing solution with a vesicle nanostructure in the quiescent state. Later Zheng et al. [7], using cryo-TEM imaging of a known drag-reducing system, Arquad 16-50/Na 3-methyl salicycle (5 mM/5 mM), showed that vesicles could transform to thread-like structures under shear and relax back to vesicles when shear was removed.

The rheological behavior under shear of drag-reducing surfactant solutions containing rod-like or thread-like micelles has been widely investigated. A variety of responses to shear have been observed with some solutions exhibiting shear thinning (orientation of micelles in the shearing direction) while others exhibit phenomena such as shear-induced structures (SIS), gelation and flow instabilities [8–12]. Lu et al. [13] reported a zero first normal stress

* Corresponding author. Fax: +1 614 292 3769.
E-mail address: zakin@chbmeng.ohio-state.edu (J.L. Zakin).

0021-9797/$ - see front matter © 2009 Elsevier Inc. All rights reserved.
doi:10.1016/j.jcis.2009.05.020

difference (N_1) solution which was drag reducing. These behaviors are of great interest, both theoretically and for practical applications [12,14–16], but the origins of these phenomena and their relationship to surfactant nanostructure are not fully understood.

Scattering methods have proven to be powerful techniques to investigate microstructural properties of various materials quantitatively on a broad range of length scales. SANS is particularly suitable for the investigation of surfactant micelles, as it can probe inhomogeneities from the near atomic scale, 1–100 nm, which covers the range of micelle diameters and, for thread-like micelles, the persistence length of the micelles. Due to its weak interaction with matter, neutrons can penetrate through matter without significant loss and this makes it possible to probe the samples contained in complex apparatuses such as shear cells, pressure cells, etc. When coupled with a shear cell, shear effects on solution nanostructures can be obtained from SANS [17,18]. SANS is thus useful in the study of drag-reducing surfactant micelle solutions, because the orientation behavior of thread-like micelles caused by shear is of particular interest.

In this paper, effects of shear on three drag-reducing surfactant solutions each with very different nanostructures and different rheological responses to shear: (1) Arquad 16-50/NaSal (5 mM/5 mM) (contains thread-like micelles, shear-induced structure (SIS), large N_1); (2) Arquad S-50/NaSal (5 mM/12.5 mM) (contains branched micelles, no SIS, $N_1 \approx 0$), and; (3) Arquad 16-50/Na 3,4-dimethyl-benzoate (5 mM/5 mM) (contains vesicles and thread-like micelles, SIS, high N_1) are explored using SANS and cryo-TEM imaging to probe the relationships among their rheological and drag-reducing behavior and their nanostructures. The differences in their rheological behavior and in their responses to shear in SANS measurements are explained by the differences in their nanostructures.

2. Experimental methods

2.1. Materials and sample preparation

The chemical structures, molecular weights and supplier of the surfactants and counterions used are listed in Table 1. Arquad S-50 is soya-alkyl-trimethyl ammonium chloride. It is made from soybean oil and is a mixture of 16- and 18-carbon chain surfactants with the following chain distribution: 10% C_{16} (saturated), 25% C_{18} (saturated), 51% C_{18} (unsaturated) and 6% C_{18} (linoleyl). The average carbon number of the chain is 17.7. The C_{18} unsaturated chain has one double-bond located between the 9th and the 10th carbons (40% *cis* and 60% *trans*), while the linoleyl chain has two double-bonds, one between the 9th and 10th and the other between the 12th and 13th carbons. This cationic surfactant system was chosen because its nanostructure differs markedly from the others and because of its unusual viscoelastic character and its Newtonian shear viscosity.

For solutions with salicylate counterions, sodium salicylate (NaSal) was first dissolved in water, except for the SANS experiments where the solvent was D_2O. The required amounts of surfactant and solvent were then added to the solution while stirring. For 3,4-dimethyl-benzoic acid, an equal molar amount of sodium hydroxide (Mallinckrodt, AR grade) was used to neutralize the acid. Otherwise the procedure was similar to that for NaSal. This surfactant/counterion system was chosen because of its vesicle nanostructure in the quiescent state which transforms to thread-like micelles under shear which is similar to that of Zheng et al. [7]. The solutions were stirred for more than 6 h, and kept at room temperature for more than 24 h after stirring to allow them to equilibrate. For drag reduction, rheological and nanostructure experiments, deionized water was used as solvent while for SANS, D_2O was used to provide better contrast between the surfactant and the solvent.

2.2. Rheology

2.2.1. Shear viscosity

Shear viscosity measurements were carried out with a Rheometrics RFSII Couette rheometer. The Couette cell had a cup diameter of 34 mm and bob diameter of 32 mm, giving a fixed gap of 1 mm. The bob length was 32 mm. The experiments were run at room temperature (20 ± 2 °C) over a shear rate range of 10–1000 s^{-1}. To ensure that the viscosities reached their equilibrium values, the solutions were sheared for 60 s at each shear rate before taking readings. The shear viscosity was calculated from the average of clockwise and counter clockwise measurements at each shear rate.

2.2.2. First normal stress difference

First normal stress differences of the solutions were measured using a Rheometric Scientific Inc. RMS-800 rheometer with a cone-and-plate fixture (50 mm diameter; cone angle of 0.04 radians). The experiments were conducted at room temperature (20 ± 2 °C) over a shear rate range of 20–800 s^{-1}. The minimum shear rate was limited by the sensitivity of the transducer, while the maximum shear rate was limited by foaming of the surfactant solutions.

All of the measured first normal stress difference results were corrected for inertial effects using Eq. (1) by Macosko [19].

$$N_{1corrected} = N_{1reading} + 0.15\rho\Omega^2 R_p^2 \quad (1)$$

ρ is the solution density, Ω is the angular velocity of the rheometer cone, and R_p is cone radius. Since the inertial force is in the opposite direction from the normal force, the correction term, $0.15\rho\Omega^2 R_p^2$, must be added to the rheometer output, giving an increasing $N_{1corrected}$ over the $N_{1reading}$.

2.3. Cryo-TEM

To take cryogenic transmission electron microscope (cryo-TEM) images of drag-reducing surfactant solutions, the samples were prepared in a controlled temperature and humidity chamber. A small drop of the studied solution is applied on a perforated carbon film supported by an electron microscope grid for cryo-TEM measurements. The drop is then blotted to a very thin liquid film with thickness of about 0.2 μm, and rapidly plunged into liquid ethane at its freezing point (~90 K) to vitrify the liquid [20,21]. Sample preparation is done at 100% relative humidity and fixed tempera-

Table 1
Cationic surfactants and counterions.

Trade name	Chemical structure	Molecular weight	Purity (%)	Supplier
Arquad S-50	Soya-$N(CH_3)_3Cl$	345.5	50[a]	Akzo Nobel
Arquad 16-50	$C_{16}H_{33}$–$N(CH_3)_3Cl$	320.0	50[a]	Akzo Nobel
Sodium salicylate	2-OH–C_6H_4–COONa	160.0	99	Aldrich Chem. Co.
3,4-Dimethyl-benzoic acid	3,4-CH_3–C_6H_3–COOH	150.2	98	Aldrich Chem. Co.

[a] In aqueous solution with 35% isopropanol.

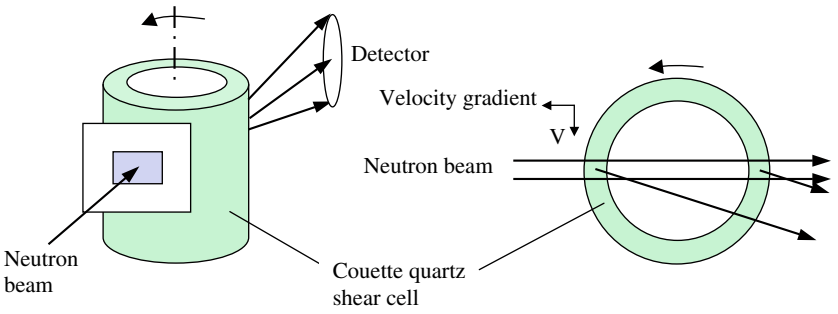

Fig. 1. Scattering geometry of Couette shear cell.

ture in a controlled vitrification system. Images of the vitrified samples were then recorded by a gatan MultiScan 791 cooled-CCD camera at nominal objective lens under focus of about 2 μm with a Philips CM120 transmission electron microscope operated at 120 kV, using an Oxford CT 3500 cooling holder operated at about −180 °C.

The whole process is designed to avoid water crystallization so that the nanostructure is not disturbed, and the images obtained reflect the true nanostructure in the original solution. However, when blotting the samples to form a thin film on the grid, the samples experience very high shear rates which may cause nanostructural transitions [7]. In addition, different portions of the film may be subjected to different intensities of shear during blotting, and, as a result, the vitrified film of the sample suspended over the perforated polymer film may have a thickness distribution after blotting of 200–400 nm near the edge and down to 10 nm in the thinner parts.

2.4. SANS measurements

SANS experiments at quiescent conditions and under shear were performed using the time-of-flight small-angle scattering instrument (SAND) at IPNS (Intense Pulsed Neutron Source) at Argonne National Laboratory which has a Q range of 0.004–0.04 $Å^{-1}$.

Samples were loaded in a quartz Couette cell with a rotational cup of high quality quartz and an aluminum bob (Fig. 1). The inner diameter of the rotating cup is 61 mm and the outer diameter of the stator is 59 mm giving a gap of 1 mm. The height of the Couette cell was 76.2 mm. The flow velocity was perpendicular to the incident neutron beam producing a velocity gradient parallel to the neutron beam. The scattered neutron patterns were recorded using a 40 cm × 40 cm area detector with a sample-to-detector distance of 2 m. Circulation fluid (ethylene glycol) was passed through the bob to maintain the desired temperature of 25 °C.

3. Results and discussion

Turbulent drag reduction experiments were conducted in a recirculation system with a 1.22 m long, 6 mm inner diameter stainless steel tube test section. Details of the system can be found in Lu [22].

Arquad 16-50/NaSal (5 mM/5 mM), Arquad S-50/NaSal (5 mM/12.5 mM) and Arquad 16-50/Na 3,4-dimethyl-benzoate (5 mM/5 mM) solutions all show good drag reduction at room temperature (20 ± 2 °C) with maximum drag reduction percentages of around 70% for the first two, and 60% for the Arquad 16-50/Na 3,4-dimethyl-benzoate (5 mM/5 mM) solution. However, the resistance to shear break-down of the micelles measured by the critical shear stress (at which drag reduction percentage drops to 50% after passing the peak) of the Arquad S-50/NaSal (5 mM/12.5 mM) solution is about three times that of the Arquad 16-50/NaSal (5 mM/5 mM) solution, and two times that of the Arquad 16-50/Na 3,4-dimethyl-benzoate (5 mM/5 mM) solution (Table 2). The high counterion ratio in the S-50 system reduces electrostatic effects allowing strong interactions between micelles and promotes a nanostructure with branches in this surfactant/counterion system, leading to resistance to shear break-down and to this surfactant's large critical wall shear stress in drag reduction experiments (see Table 2) [23].

3.1. Rheological properties and cryo-TEM

3.1.1. Shear viscosity

Fig. 2 shows the shear viscosities of the three drag-reducing surfactant solutions at room temperature (20 ± 2 °C). Both the Arquad 16-50/NaSal (5 mM/5 mM), which is initially shear thinning at low shear rates, and the Arquad 16-50/Na 3,4-dimethyl-benzoate (5 mM/5 mM) solutions exhibited behavior typical of shear-induced structures (SIS) in the shear rate range of 10–1000 s^{-1}, while the Arquad S-50/NaSal (5 mM/12.5 mM) solution was nearly Newtonian. The shear rate at the onset of shear thickening or shear-induced structure (SIS) of the Arquad 16-50/NaSal (5 mM/5 mM) solution was around 40 s^{-1} which was lower than the value of about 80 s^{-1} observed for the Arquad 16-50/Na 3,4-dimethyl-benzoate (5 mM/5 mM) solution. The Newtonian behavior of the latter at low shear rates suggests that its micellar structure is dominated by spherical micelles and vesicles until SIS are formed. A number of vesicles are seen in its cryo-TEM image in Fig. 4c. The thread-like

Table 2
Comparison of critical shear rates for the initialization of SIS and N_1, drag reduction critical wall shear stress at room temperature 20 ± 2 °C and the critical shear rate required to produce an anisotropic 2D SANS scattering pattern for Arquad 16-50/NaSal (5 mM/5 mM), Arquad S-50/NaSal (5 mM/12.5 mM) and Arquad 16-50/Na 3,4-dimethyl-benzoate (5 mM/5 mM) solutions.

	Critical shear rates for the initialization of SIS (s^{-1})	Critical shear rates for the initialization of N_1 (s^{-1})	Critical shear rate required to produce an anisotropic 2D SANS scattering pattern (s^{-1})	Critical wall shear stress of DR at room temperature (Pa)
Arquad 16-50/NaSal (5 mM/5 mM)	40	Less than 25	Less than 0.1	90
Arquad S-50/NaSal (5 mM/12.5 mM)	NA	NA	~29	275
Arquad 16-50/Na 3,4-dimethyl-benzoate (5 mM/5 mM)	80	90	~10	135

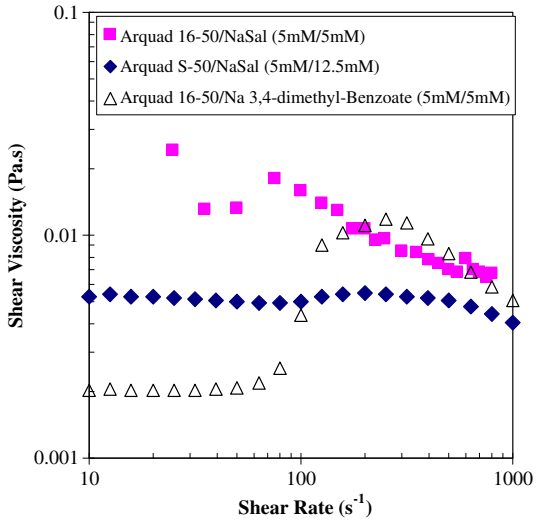

Fig. 2. Shear viscosity of drag reducing surfactant solutions Arquad 16-50/NaSal (5 mM/5 mM), Arquad S-50/NaSal (5 mM/12.5 mM) and Arquad 16-50/Na 3,4-dimethyl-benzoate (5 mM/5 mM) at room temperature.

micelles observed by cryo-TEM (both Fig. 4c and d) are then a result of shearing of the sample when it is blotted during sample preparation as observed by Zheng et al. [7].

3.1.2. First normal stress difference (N_1)

First normal stress difference (N_1) of surfactant solutions is a rheological property often studied to determine its possible relation to drag reduction ability [24]. Most drag-reducing surfactant solutions exhibit viscoelastic properties in the forms of non-zero first normal stress difference (N_1), quick recoil and stress overshoot. The N_1 data for Arquad 16-50/NaSal (5 mM/5 mM), Arquad S-50/NaSal (5 mM/12.5 mM) and Arquad 16-50/Na 3,4-dimethyl-benzoate (5 mM/5 mM) drag-reducing surfactant solutions in the shear rate range of 20–800 s^{-1} are shown in Fig. 3.

The first normal stress difference of the Arquad 16-50/NaSal (5 mM/5 mM) solution increases with shear rate reaching 350 Pa at 630 s^{-1}, indicating its strong viscoelastic nature. Its quick recoil after stirring was stopped (1.1 s) confirmed this. Surprisingly, first zero and then negative N_1 values were found for the Arquad S-50/NaSal (5 mM/12.5 mM) solution. We believe the negative values

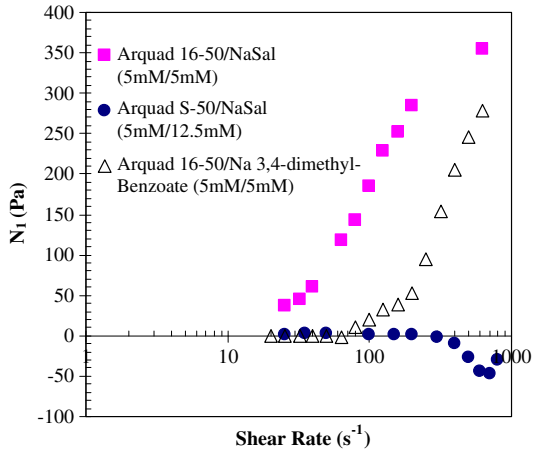

Fig. 3. First normal stress differences of drag reducing surfactant solutions Arquad 16-50/NaSal (5 mM/5 mM), Arquad S-50/NaSal (5 mM/12.5 mM) and Arquad 16-50/Na 3,4-dimethyl-benzoate (5 mM/5 mM) at room temperature.

are due to instrument limitations. In addition, this solution showed no recoil and no shear-induced structure in its shear viscosity vs. shear rate plot in the shear rate range of 10–1000 s^{-1} (Fig. 2). The first normal stress difference of the Arquad 16-50/Na 3,4-dimethyl-benzoate (5 mM/5 mM) solution was around zero at shear rates below 90 s^{-1}. However, above 90 s^{-1}, N_1 monotonically increased and reached a value of over 250 Pa at 630 s^{-1}. It also showed quick recoil after stirring was stopped (1.2 s). The initiation of growth of N_1 values for these two solutions roughly coincided with the initiation of SIS while the S-50 solution showed neither SIS nor N_1.

3.1.3. Cryo-TEM images

The cryo-TEM images (Fig. 4) of the vitrified surfactant solutions show long flexible thread-like micelles present in all three drag-reducing surfactant solutions with diameters of about 5 nm and contour lengths much greater than 100 nm. For Arquad 16-50/Na 3,4-dimethyl-benzoate (5 mM/5 mM) surfactant solution, vesicles were also found in the solution, coexisting with thread-like micelles (TLMS; see Fig. 4c). Fig. 4d is another view of the same solution. The existence of vesicles in this solution may contribute to lowering the viscoelasticity and shear viscosity of the solution at low shear rates. According to Mendes and Menon [5], Mendes et al. [6] and Zheng et al. [7], vesicles can transform to thread-like micelles under shear due to counterion re-distribution in the solution.

Interactions between thread-like micelles are the causes of the viscoelasticity of the surfactant solutions. Thus, it is surprising that the Aquad S-50/NaSal (5 mM/12.5 mM) solution exhibited zero first normal stress differences and no recoil, even though long thread-like micelles were present in the solution (Fig. 4b). However, the Arquad S-50 solution thread-like micelle structure is different as it has branches and loops. Chellamuthu and Rothstein [23] stated that "Branches may allow two entangled micelles to pull right through each other thereby eliminating the entanglement point and relieving stress in what has become known as a "ghost-like" crossing." Thus, these branched systems are accompanied by higher resistance to shear degradation and also lower viscosity, a phenomenon reported earlier [25].

The differences in the rheological properties of the surfactant solutions imply differences in their nanostructures. However, since cryo-TEM images of the surfactant solutions (Fig. 4) represent a snapshot of the surfactant solutions at a single moment after blotting, and it is not possible to quantitatively control the shear conditions when blotting the sample, it is difficult to tell in detail from these images how the surfactant nanostructures change with shear rate, although the careful experiments by Zheng et al. [7] clearly showed the structural changes from vesicles to threads of the Arquad 16-50/Na 3-methyl salicylate system and their relaxation back to vesicles when shear was removed. Therefore, small-angle neutron scattering (SANS) experiments were carried out to study the effect of shear on the nanostructures of these three drag-reducing surfactant solutions and to relate them to the rheological behavior of the three systems.

3.2. Small-angle neutron scattering (SANS)

3.2.1. 2D SANS patterns

The anisotropic patterns in 2D SANS can be used to study how thread-like micellar systems respond to shear. The 2D SANS scattering patterns of the three solutions at different shear rates are shown in Figs. 5–7. For the Arquad 16-50/NaSal (5 mM/5 mM) solution (Fig. 5), an isotropic scattering ring is observed at zero shear rate, indicating isotropic ordering of the thread-like micelles in the quiescent solution. At a shear rate of 10 s^{-1} in the Couette shear cell, alignment of the thread-like micelles along the flow

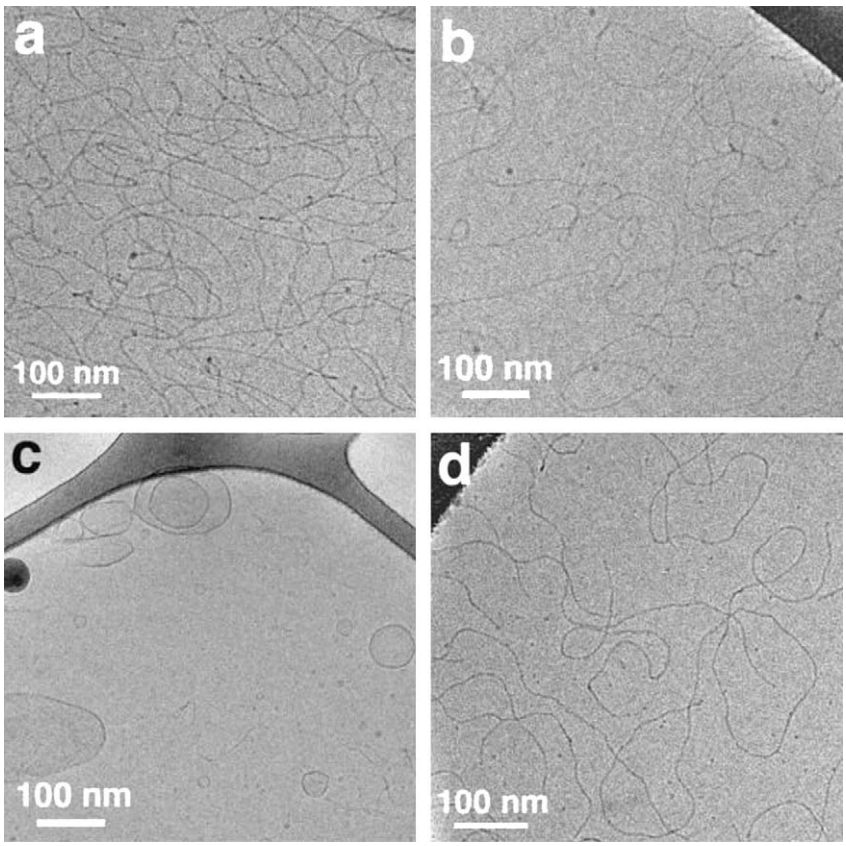

Fig. 4. Cryo-TEM images of drag reducing surfactant solutions. (a) Arquad 16-50/NaSal (5 mM/5 mM); (b) Arquad S-50/NaSal (5 mM/12.5 mM); (c and d) Arquad 16-50/Na 3,4-dimethyl-benzoate (5 mM/5 mM) at room temperature.

direction is seen as evidenced by the anisotropic scattering pattern of the solution with the scattering intensity decreasing parallel to the flow direction and increasing in the direction perpendicular to the flow (the neutral direction). With further increase of shear rate above 10 s^{-1}, up to the highest shear rate of 2000 s^{-1}, the anisotropic scattering pattern did not change appreciably. This indicates that the micelles had already reached nearly full alignment at a shear rate of around 10 s^{-1}. At much larger shear rates it is expected that the thread-like micelles will break up due to the high shear stress, and the SANS pattern will become isotropic. However, SANS patterns did not become isotropic even at shear rates above 3000 s^{-1} (not shown in Fig. 5).

The 2D SANS patterns of Arquad S-50/NaSal (5 mM/12.5 mM) solution at different shear rates are shown in Fig. 6. In contrast to the Arquad 16-50/NaSal (5 mM/5 mM) solution, scattering patterns were less anisotropic for this system. Even at the maximum shear rate of 3000 s^{-1}, the scattering pattern of Arquad S-50/NaSal (5 mM/12.5 mM) solution (Fig. 6) was not as anisotropic as that of Arquad 16-50/NaSal (5 mM/5 mM) solution at 10 s^{-1} (Fig. 5). Thus, it appears that the branched Arquad S-50/NaSal (5 mM/12.5 mM) solution threads are not fully aligned even at a shear rate of 3000 s^{-1}. The dramatically different responses of the micelles in these solutions indicate that the morphologies of micelles in these two solutions are quite different such as different persistence lengths. Here persistence length is used to characterize the stiffness of the thread-like micelles. It is defined as the length over which the cylindrical micelle can be considered as rigid [26,27].

Fig. 7 displays SANS 2D patterns of Arquad 16-50/Na 3,4-dimethyl-benzoate (5 mM/5 mM) solution in the shear rate range of 0–3000 s^{-1}. The isotropic scattering ring pattern persisted up to a shear rate of 10 s^{-1}. When shear rate was increased to 100 s^{-1}, the scattering pattern turned into an ellipse with its long axis aligned perpendicular to the flow direction. At 1000 s^{-1}, it became more anisotropic. No substantial change was observed when the shear rate was increased to 3000 s^{-1}. The scattering pattern of this solution at a shear rate of 100 s^{-1} resembled the pattern of Arquad S-50/NaSal (5 mM/12.5 mM) solution at shear rates of 2000–3000 s^{-1}, while those measured at 1000 s^{-1} and 3000 s^{-1} are closer to those of the Arquad 16-50/NaSal (5 mM/5 mM) solution in the shear rate range of 10–2000 s^{-1}.

Thus, for Arquad 16-50/Na 3,4-dimethyl-benzoate (5 mM/5 mM) solution, the critical shear rate required to produce an anisotropic scattering pattern was above 10 s^{-1} (Fig. 7) which is larger than that of the Arquad 16-50/NaSal (5 mM/5 mM) solution, but much smaller than the critical shear rate of the Arquad S-50/NaSal (5 mM/12.5 mM) solution. The shear rate needed to fully align the thread-like micelles is much higher for Arquad S-50/NaSal (5 mM/12.5 mM) solution than for Arquad 16-50/Na 3,4-dimethyl-benzoate (5 mM/5 mM) and Arquad 16-50/NaSal (5 mM/5 mM).

Anisotropic ratios of the SANS 2D patterns vs. shear rate are plotted in Fig. 8. The anistropic ratio is the ratio of the vertical (90°) length minus the horizontal (0°) length of the 2D SANS pattern to the 90° length. It typically ranges from 0 to near 0.8. The Arquad 16-50/NaSal (5 mM/5 mM) system rises rapidly above 1 s^{-1}, reaching a value of 0.5 at 4 s^{-1} while the Arquad 16-50/Na 3,4-dimethyl-benzoate (5 mM/5 mM) data rise rapidly above 10 s^{-1} to reach a ratio of 0.5 at 100 s^{-1}. In the case of Arquad S-50/NaSal (5 mM/12.5 mM) the ratio does not reach 0.5 until about 3000 s^{-1}. The other two systems reach a limiting value of 0.75 at high shear rate, close to the limiting value for the equimolar allyl-hexadecyldimethyl ammonium bromide/NaSal system reported by

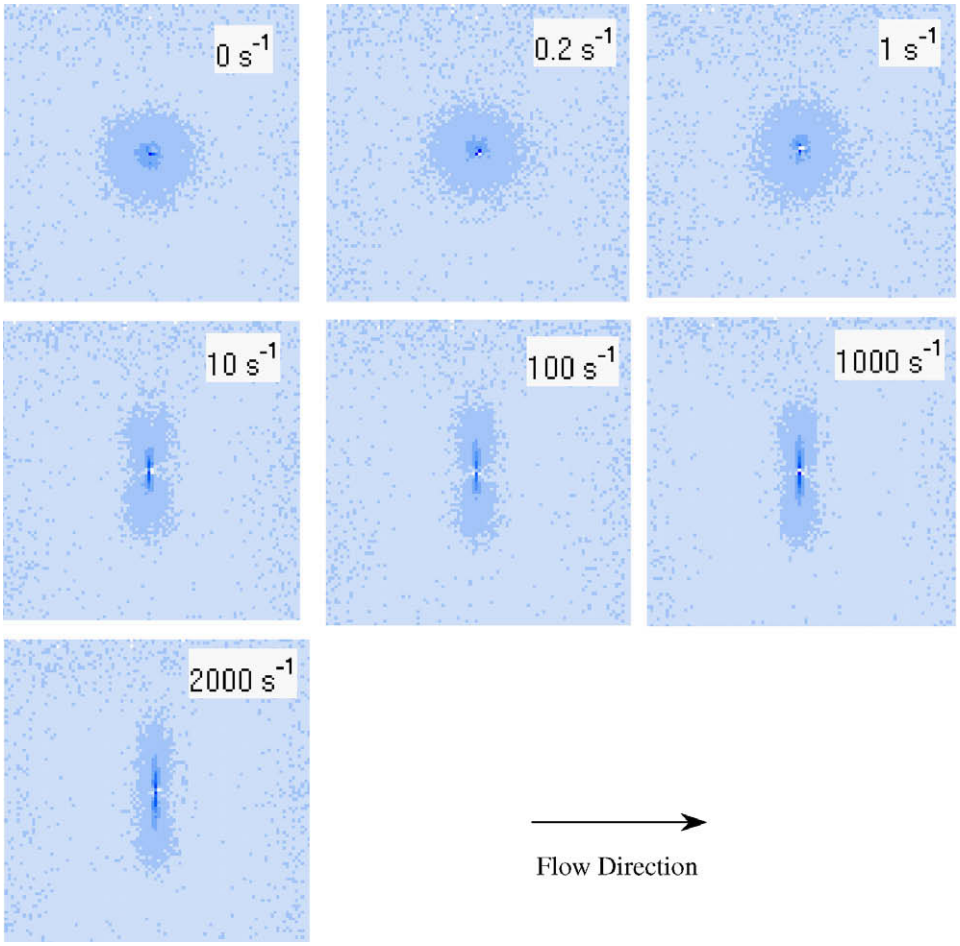

Fig. 5. SANS 2D plots of Arquad 16-50/NaSal (5 mM/5 mM) drag reducing surfactant solution at different shear rates at room temperature.

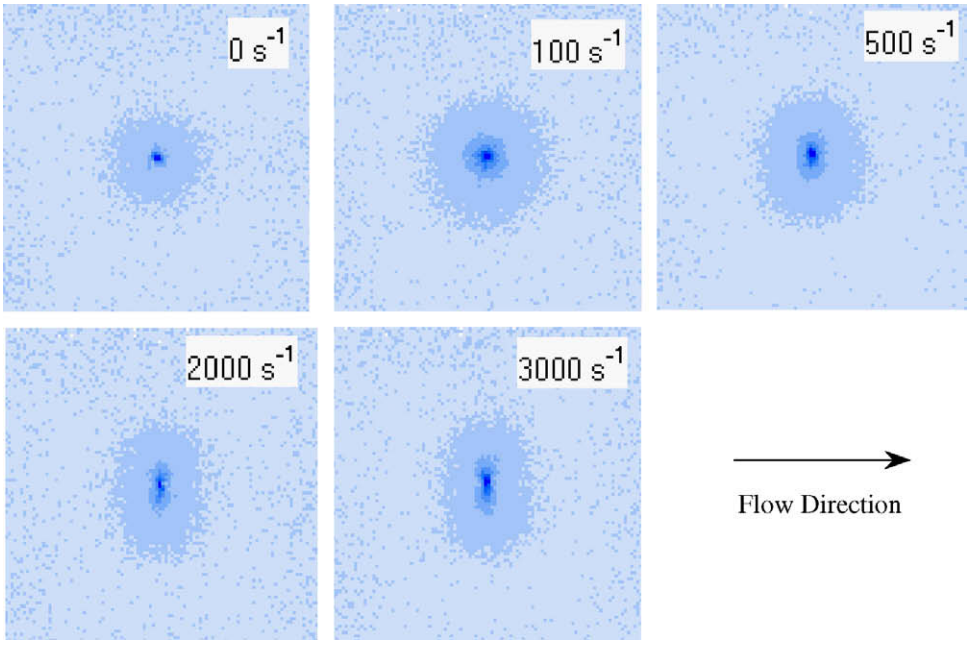

Fig. 6. SANS 2D plots of Arquad S-50/NaSal (5 mM/12.5 mM) drag reducing surfactant solution at different shear rates at room temperature.

Lin et al. [28]. This ratio presumably reflects complete alignment of the thread-like micelles for these systems.

Table 2 lists approximate critical shear rates for the initiation of SIS and N_1 and for 2D SANS anisotropy for each of the solutions.

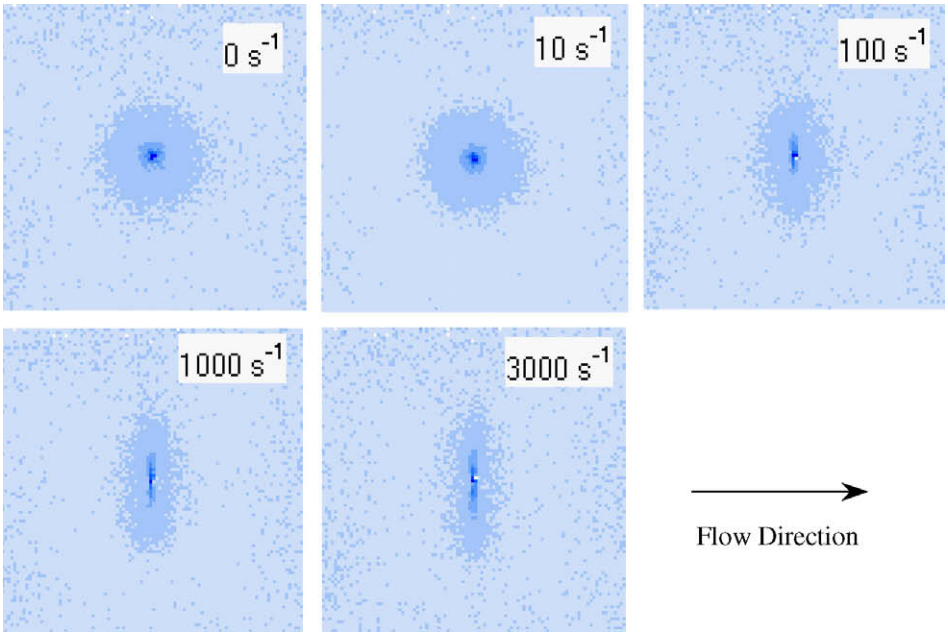

Fig. 7. SANS 2D plots of Arquad 16-50/Na 3,4-dimethyl-benzoate (5 mM/5 mM) drag reducing surfactant solution at different shear rates at room temperature.

The critical shear rates for SIS and N_1 in each case are roughly equal. The initiation of the SANS 2D anisotropy occurs at a much lower shear rate. These results are consistent with the critical wall shear stresses for micelle break-down of the three solutions obtained from drag reduction experiments at room temperature (see Table 2), where the critical wall shear stress of the Arquad S-50/NaSal (5 mM/12.5 mM) solution was found to be three times that of the Arquad 16-50/NaSal (5 mM/5 mM) solution, and twice that of the Arquad 16-50/Na 3,4-dimethyl-benzoate (5 mM/5 mM) solution.

Although thread-like micelles are found in both the Arquad 16-50/NaSal (5 mM/5 mM) and the Arquad S-50/NaSal (5 mM/12.5 mM) solutions, as shown in Fig. 4, based on the differences in their rheological behavior and SANS scattering patterns under shear, their morphologies are quite different. The branched Arquad S-50 is a mixture of surfactants of different alkyl chain lengths (C_{16} and C_{18}) and different configurations (saturated and unsaturated, *cis* and *trans*, with one and two double-bonds), with an average carbon number of 17.7, larger than the carbon number of 16 in Arquad 16-50 (Table 1). Therefore, even at the same counterion concentration, the structure of Arquad S-50 is more favorable for micellar growth than that of Arquad 16-50, due to the stronger hydrophobic interactions between its longer alkyl chains. In addition, the unsaturated double-bond surfactants such as *cis* and *trans* with 18 carbons in the Arquad S-50 quaternary ammonium salt mixed surfactant favor micellar growth according to the packing parameter analysis by Israelachivili [29], because of their reduced extended hydrocarbon chain length so we should expect its response to shear to be different than the other systems.

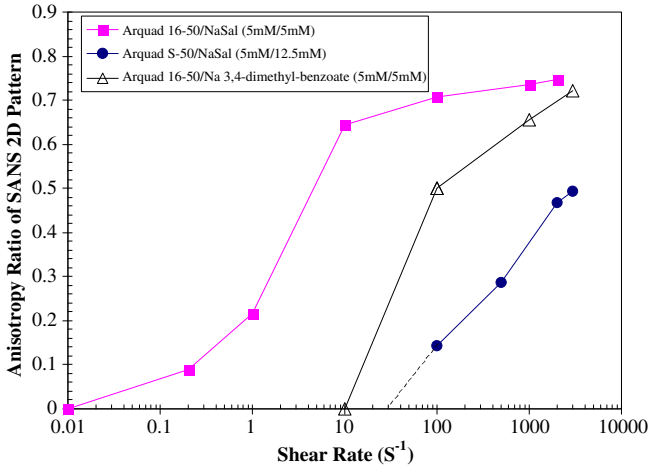

Fig. 8. Anisotropic ratio of SANS 2D pattern for Arquad 16-50/NaSal (5 mM/5 mM), Arquad S-50/NaSal (5 mM/12.5 mM) and Arquad 16-50/Na 3,4-dimethyl-benzoate (5 mM/5 mM) solutions at room temperature.

Also, the counterion concentration in Arquad S-50/NaSal (5 mM/12.5 mM) solution is 2.5 times that of the Arquad 16-50/NaSal (5 mM/5 mM) solution. The larger counterion concentration in the Arquad S-50/NaSal (5 mM/12.5 mM) solution not only decreases the electrostatic interactions between the micelles but also decreases the self-repulsion of a thread-like micelle along its length [30–33] and favors branch formation [34]. Therefore, the branched thread-like micelles formed in Arquad S-50/NaSal (5 mM/12.5 mM) solution are expected to be larger, more flexible and with a shorter persistence length (more curvature between entangling points) than the thread-like micelles in the Arquad 16-50/NaSal (5 mM/5 mM) solution.

Butler et al. [31] and Hamilton et al. [32] pointed out that for surfactant solutions with very flexible thread-like micelles such as Arquad S-50/NaSal (5 mM/12.5 mM), there are two steps in the shearing alignment process along the flow direction. The first step is a local deformation (stretching) of the network, resulting in alignment of micellar segments over a length scale roughly equivalent to the distance between entanglement points. The effect of this alignment process on the anisotropy of the scattering pattern at a given shear rate depends strongly on the persistence length of the thread-like micelles. The shorter the persistence length, the more flexible the thread-like micelles, with more curves along the micelle segment between two entangling points requiring a higher shear rate to align the micelle segments between two entangling points along the flow direction. During this step, a slight anisotropic scattering pattern will be observed as shown in Fig. 6 at shear rates of 500 s^{-1}, 2000 s^{-1} and 3000 s^{-1}. The second step in this process is the large-scale disentanglement and

alignment of the individual thread-like micelles along the flow direction. When this step starts, the scattering pattern of the surfactant solutions will become very anisotropic as seen in the scattering patterns of Arquad 16-50/NaSal (5 mM/5 mM) solution at shear rates greater than 10 s^{-1} (Fig. 5). Since for solutions with small electrostatic repulsion between micelles like the Arquad S-50/NaSal (5 mM/12.5 mM) the chances for transient contacts between micelles are large and the second step becomes more difficult, full alignment of micelles in this solution is not observed even at a shear rate of 3000 s^{-1}.

The scattering pattern of the Arquad 16-50/3,4-dimethyl-benzoate (5 mM/5 mM) solution at 100 s^{-1} (Fig. 7) is more anisotropic than that of the Arquad S-50/NaSal (5 mM/5 mM) solution at shear rates of 500 s^{-1}, 2000 s^{-1} and 3000 s^{-1} (Fig. 6), but is not as anisotropic as that of the Arquad 16-50/NaSal (5 mM/5 mM) solution at shear rates above 10 s^{-1} (Fig. 6). The large-scale disentanglement and alignment of individual thread-like micelles in this solution start around 10 s^{-1} (Figs. 7 and 8). At a shear rate of about 80 s^{-1} this solution begins to show SIS (Fig. 2) and positive N_1 values at 90 (Fig. 3). For Arquad S-50/NaSal (5 mM/12.5 mM) solution, which apparently does not undergo the second alignment step in the shear rate range studied, the observed N_1 values are zero at shear rates up to 400 s^{-1} above which they become negative (Fig. 3) and no SIS is observed up to 1000 s^{-1}, supporting the postulate that surfactant solutions with thread-like micelles exhibit non-zero N_1 only when the second step alignment, revealed by the strongly anisotropic scattering patterns, occurs.

For surfactant solutions with shorter, less flexible and strongly interacting thread-like micelles (stronger electrostatic repulsion forces) such as Arquad 16-50/NaSal (5 mM/5 mM), the first alignment step readily occurs at low shear rates (less than 10 s^{-1}), and the second step, large-scale disentanglement and alignment of individual thread-like micelles along the flow direction, dominates at shear rates above 10 s^{-1}. With its strongly anisotropic scattering pattern at a shear rate of 10 s^{-1} (Fig. 5), non-zero first normal stress difference (N_1) was detected at the lowest measurable shear rate, 20 s^{-1}, further supporting the argument that non-zero N_1 is associated with the second alignment process.

The critical shear rate for SIS of Arquad 16-50/NaSal (5 mM/5 mM) solution is around 40 s^{-1} which is larger than the anisotropic scattering pattern shear rate, 10 s^{-1} or less (Fig. 8). This result agrees with the theories suggesting that the shear-thickening behavior of a surfactant solution with thread-like micelles is caused by the enhanced rate of collision and collinear fusion between aligned and extended thread-like micelles in the flow field [35–40] and the critical shear rate for SIS should be larger than that for the anisotropic scattering pattern. However, it does not agree with that of Oda et al. [41] who proposed that for surfactant solutions exhibiting shear-induced structure, the anisotropic scattering pattern appears only at shear rate values larger than the critical shear rate for shear-induced structure, i.e., the onset of shear thickening. The decrease in shear viscosity with shear rate at shear rates below 40 s^{-1} in Fig. 2 is also consistent with the thread-like micelles in the Arquad 16-50/NaSal (5 mM/5 mM) solution starting to align along the flow direction below a shear rate of 25 s^{-1}.

The critical shear rate for Arquad 16-50/Na 3,4-dimethyl-benzoate (5 mM/5 mM) solution to exhibit an anisotropic scattering pattern starts at 10 s^{-1} (Figs. 7 and 8), and the critical shear rate for SIS of the solution is around 80 s^{-1}, as shown in Fig. 2 again contradicting Oda et al. [41]. Thus, for the Arquad 16-50/NaSal (5 mM/5 mM) and the Arquad 16-50/Na 3,4-dimethyl-benzoate (5 mM/5 mM) solutions, shear-induced structure of the surfactant solutions starts either during the first alignment step of stretching the micelle segments between the entangling points, or possibly at the second step with large-scale disentanglement and alignment of individual micelles along the flow direction. For the more flexible Arquad S-50/NaSal (5 mM/12.5 mM) solution, no SIS was observed in the shear rate range of 10–1000 s^{-1}, and only slight anisotropy even at 2000 s^{-1}. Thus, the two-step shear alignment process proposed by Butler et al. [31] and Hamilton et al. [32] explains the differences in the SIS, N_1, and SANS results for the Arquad S-50 micellar system from the results for the other two systems.

4. Summary

Due to the differences in the hydrocarbon chain composition and counterion concentrations, three drag-reducing surfactant solutions (Arquad 16-50/NaSal (5 mM/5 mM), Arquad S-50/NaSal (5 mM/12.5 mM) and Arquad 16-50/Na 3,4-dimethyl-benzoate (5 mM/5 mM)) show different rheological behavior and SANS 2D patterns. The differences in drag reduction, rheological behavior and SANS 2D scattering patterns are consistent and can be explained by differences in their nanostructure responses to shear following a two-step shear response.

Based on the results, small lab. scale tests of the rheological properties of drag-reducing candidate systems can be used to rank the critical wall shear stress for loss of drag reduction, a very useful screening tool for new formulations.

1. In a Couette shear cell, thread-like micelles in drag-reducing surfactant solutions align with their long axes along the flow direction as evidenced by the anisotropic SANS 2D scattering patterns of the solutions under shear. The degree of anisotropy of scattering patterns at a certain shear rate is strongly related to the different nanostructures of the three surfactant systems studied. A much higher shear rate is needed to fully align the branched micelles in the Arquad S-50/NaSal (5 mM/12.5 mM) solution than for the Arquad 16-50/NaSal (5 mM/5 mM) and the Arquad 16-50/Na 3,4-dimethyl-benzoate (5 mM/5 mM) solutions. This result is consistent with their SIS, their N_1 and their critical wall shear stress for loss of drag reduction behavior of the three solutions.
2. Due to the differences in the hydrocarbon chain configurations and counterion concentrations in Arquad 16-50/NaSal (5 mM/5 mM) and Arquad S-50/NaSal (5 mM/12.5 mM) solutions, and the higher NaSal to surfactant ratio, the thread-like micelles in the latter solution are branched, longer and more flexible with shorter persistence length and more curvature between entangling points than the former, accounting for the different responses to shear, rheological properties and scattering patterns of the two solutions. It follows that the latter, more shear resistant system, has much higher critical wall shear stress for loss of drag reduction.
3. Based on the zero or negative N_1 of the Arquad S-50/NaSal (5 mM/12.5 mM) solution over a shear rate range of 20–1000 s^{-1} and Arquad 16-50/Na 3,4-dimethyl-benzoate (5 mM/5 mM) solution at shear rates below 90 s^{-1}, it is postulated that for surfactant solutions with thread-like micelles to exhibit N_1, the shear rate has to be large enough for their thread-like micelles to start the second alignment step proposed by Butler et al. [30] and Hamilton et al. [31]. The strong anisotropic SANS 2D scattering patterns found in Arquad 16-50/NaSal (5 mM/5 mM) solution at shear rates above 10 s^{-1} and in Arquad 16-50/Na 3,4-dimethyl-benzoate (5 mM/5 mM) solution above 100 s^{-1} are accompanied by positive N_1 values.
4. For surfactant solutions exhibiting shear-thickening behavior, SIS might occur at either the first or the second step of the alignment process. According to the theory that SIS is caused by the collinear collision and fusion between aligned thread-like micelles., it is more reasonable that the critical shear rate for

SIS be higher than that for the anisotropic scattering pattern of the solution as found in our two Arquad 16-50 solutions, contradicting a report by Oda et al. [40], in which they found the critical shear rate for SIS to be lower than that required to produce an anisotropic scattering pattern have.

5. The vesicle-to-micelle transition observed in the cryo-TEM image of Arquad 16-50/16-50/Na 3-methyl salicylate (5 mM/5 mM) solution at room temperature by Zheng et al. [7] can explain the low shear viscosity of the Arquad 16-50/Na 3,4-dimethyl benzoate (5 mM/5 mM) solution at low shear rate (Fig. 2). These vesicle nanostructures transform to thread-like micelles under sufficient shear, enabling the solution to be drag reducing. From Fig. 8, the vesicle-to-thread-like micelles transformation appears to start at a shear rate above 10 s^{-1} while SIS begins at about 80 s^{-1}.

Acknowledgments

Y. Qi appreciates the support of a University Fellowship and a Presidential Fellowship from The Ohio State University. This work benefitted from the use of IPNS, supported by DOE-BES under Contract #DEFG0296ER45612 to the University of Chicago. The authors wish to thank Mr. Denis Wozniak in IPNS of Argonne National Laboratory for his kind help in the small-angle neutron scattering experiments. The cryo-TEM work was performed at the Hannah and George Krumholz Advanced Microscopy Laboratory, part of the Technion Project on Complex Fluids, Microstructure and Macromolecules. The Technion group's research was supported in part by The Fund for Promotion of Research at the Technion.

References

[1] J.L. Zakin, B. Lu, H.W. Bewersdorff, Rev. Chem. Eng. 14 (1998) 253.
[2] J.L. Zakin, Y. Zhang, W. Ge, Giant Micelles: Properties and Applications, CRC Press Taylor and Francis Group, New York, 2007.
[3] J.F. Berret, R. Gamey-Corrales, J. Oberdidde, L.M. Walker, P. Lindner, Europhys. Lett. 41 (1998) 677.
[4] J.F. Berret, R. Gamey-Corrales, Y. Senero, F. Moliner, P. Lindner, Europhys. Lett. 54 (2001) 605.
[5] E. Mendes, S.V.G. Menon, Chem. Phys. Lett. 275 (1997) 477.
[6] E. Mendes, J. Narayanan, R. Oda, F. Kern, S.J. Candau, J. Phys. Chem. B 101 (1997) 2256.
[7] Y. Zheng, Z. Lin, J.L. Zakin, Y. Talmon, H.T. Davis, L.E. Scriven, J. Phys. Chem. B 104 (2000) 5263.
[8] V. Hartmann, R. Cressely, Rheol. Acta 37 (1998) 115.
[9] J. Myska, P. Stern, Colloid Polym. Sci. 276 (1998) 816.
[10] R. Oda, P. Panizza, M. Zchmutz, F. Lequeux, Langmuir 13 (1997) 6407.
[11] P. Fischer, Rheol. Acta 39 (2000) 234.
[12] P.D. Butler, Curr. Opin. Colloid Interface Sci. 4 (1999) 214.
[13] B. Lu, X. Li, J.L. Zakin, Y. Talmon, J. Non-Newtonian Fluid Mech. 71 (1997) 59.
[14] S. Hofmann, H. Hoffmann, J. Phys. Chem. B 102 (1998) 5614.
[15] P. Sullivan, E. Nelson, V. Anderson, T. Hughes, Giant Micelles: Properties and Applications, CRC Press, Taylor and Francis Group, New York, 2007.
[16] L. Nicolas-Morgantimi, Giant Micelles: Properties and Applications, CRC Press, Taylor and Francis Group, New York, 2007.
[17] J. Kalus, H. Hoffman, J. Chem. Phys. 87 (1) (1987) 714.
[18] H.J. Hanley, Curr. Opin. Colloid Interface Sci. 2 (1997) 635.
[19] C.W. Macosko, Rheology: Principles, Measurements, and Applications, VCH, New York, 1994.
[20] Y. Talmon, Ber. Bunsenges. Phys. Chem. 100 (3) (1996) 364.
[21] Y. Talmon, Giant Micelles: Properties and Applications, CRC Press, Taylor and Francis Group, New York, 2007.
[22] B. Lu, Characterization of drag reducing surfactant systems by rheology and flow birefringence measurements, Ph.D. Dissertation, The Ohio State University, Columbus, 1997.
[23] M. Chellamuthu, J.P. Rothstein, J. Rheol. 52 (3) (2008) 865.
[24] Y. Qi, J.L. Zakin, Ind. Eng. Chem. Res. 4 (2002) 6326.
[25] S.R. Raghavan, G. Fritz, E.W. Kaler, Langmuir 18 (2002) 3797.
[26] M.E. Cates, S.J. Candau, J. Phys. Condens. Matter 2 (1990) 6869.
[27] J. Appell, G. Porte, J. Colloid Interface Sci. 87 (2) (1982) 492.
[28] M.Y. Lin, H.J.M. Hanley, S.K. Sinha, G.C. Straty, D.G. Peiffer, M.W. Kim, Phys. Rev. E 53 (6) (1996) 53.
[29] J. Israelachivili, Intermolecular and Surface Forces, Academic Press, Harcourt Brace & Company, 1992.
[30] S.R. Raghavan, E.W. Kaler, Langmuir 17 (2001) 300.
[31] P.D. Butler, L.J. Magid, W.A. Hamilton, J.B. Hayter, B. Hammouda, P.J. Kreke, J. Phys. Chem. 100 (1996) 442.
[32] W.A. Hamilton, P.D. Butler, John B. Hayter, L.J. Magid, P.J. Kreke, Physica B (Amsterdam, Neth.) 221 (1996) 309.
[33] L.J. Magid, Z. Han, Z. Li, P. D Butler, J. Phys. Chem. B 104 (2000) 6717.
[34] Y. Zhang, Correlations Among Surfactant Drag Reduction, Additive chemical structures, rheological properties and microstructures in water and water/colvent systems, Ph.D. Dissertation, Ohio State University, Columbus, 2005.
[35] S. Hofmann, H. Hoffmann, J. Phys. Chem. B 102 (1998) 5614.
[36] M.E. Cates, M.S. Turner, Europhys. Lett. 11 (7) (1990) 681.
[37] M.S. Turner, M.E. Cates, J. Phys: Condens. Matter 4 (1992) 3719.
[38] M.E. Cates, Phil. Trans. R. Soc. Lond. A 344 (1993) 339.
[39] H. Rehage, H. Hoffmann, J. Phys. Chem. 92 (1988) 4712.
[40] R. Cressely, V. Hartmann, Eur. Phys. J. B 6 (1998) 57.
[41] R. Oda, V. Weber, P. Lindner, D.J. Pine, E. Mendes, F. Schosseler, Langmuir 16 (2000) 4859.